
Diffusion Models for Time Series Forecasting: A Survey

Chen Su^{♠†}, Zhengzhou Cai^{◇†}, Yuanhe Tian[♥], Zihong Zheng[♠], Yan Song[♠]

[♠]University of Science and Technology of China

[◇]Beijing University of Posts and Telecommunications

[♥]University of Washington

[♠]suchen4565@mail.ustc.edu.cn [◇]ai@bupt.edu.cn [♥]yhtian@uw.edu

[♠]leozheng06@mail.ustc.edu.cn [♠]clksong@gmail.com

Abstract

Diffusion models, initially developed for image synthesis, demonstrate remarkable generative capabilities. Recently, their application has expanded to time series forecasting (TSF), yielding promising results. In this survey, we firstly introduce the standard diffusion models and their prevalent variants, explaining their adaptation to TSF tasks. We then provide a comprehensive review of diffusion models for TSF, paying special attention to the sources of conditional information and the mechanisms for integrating this conditioning within the models. In analyzing existing approaches using diffusion models for TSF, we provide a systematic categorization and a comprehensive summary of them in this survey. Furthermore, we examine several foundational diffusion models applied to TSF, alongside commonly used datasets and evaluation metrics. Finally, we discuss current limitations in these approaches and potential future research directions. Overall, this survey details recent progress and future prospects for diffusion models in TSF, serving as a reference for researchers in the field.¹

Keywords Time Series Forecasting, Diffusion Models, Conditional Diffusion, Survey

1 Introduction

Time series forecasting (TSF) is a fundamental task that aims to predict future values of a sequence based on historical data. It plays a vital role in a wide range of real-world applications, such as energy demand forecasting [1, 2, 3], traffic flow prediction [4, 5, 6], and healthcare monitoring [7, 8, 9]. Time series data present diverse structures, ranging from univariate sequences that monitor a single variable over time, to multivariate sequences capturing interactions among multiple variables, as well as more complex forms such as spatio-temporal data from geo-distributed sensors and multimodal sequences that combine temporal signals with text, images, or metadata. TSF approaches undergo a significant evolution, progressing from conventional statistical models such as autoregressive integrated moving average model (ARIMA) [10, 11] and exponential smoothing [12, 13, 14] to deep learning approaches such as recurrent neural networks (RNNs) [15, 16, 17], convolutional neural networks (CNNs) [18, 19, 20], and Transformers [21, 22, 23], where the deep learning based models are widely used in nowadays research.

Among different deep learning approaches, generative ones rise in recent years with various representative models, including variational autoencoders (VAEs) [24, 25, 26], generative adversarial networks

[†]These authors contributed equally.

¹Resources are available at <https://github.com/synlp/TSF-Diff-Review>.

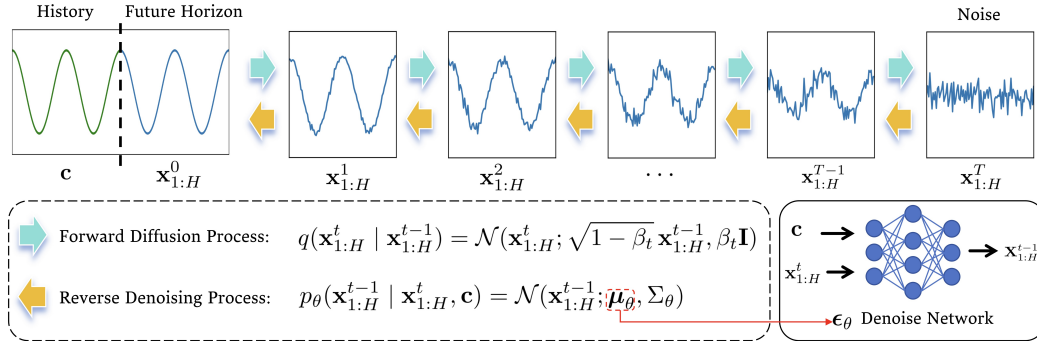


Figure 1: General approach of diffusion-based TSF.

(GANs) [27, 28, 29], and especially diffusion models [30, 31, 32, 33, 34] attract growing interest for their ability to capture uncertainty and produce high-quality forecasts. Particularly, diffusion models, as latent variable generators, learn complex data distributions through a two-step cycle of progressive noising followed by reverse denoising. This paradigm revolutionizes computer vision, enabling high-fidelity image synthesis, inpainting, and super-resolution without the adversarial instability of GANs. Motivated by such success, diffusive modeling migrates from vision to other scenarios, including TSF, and provides a generative framework for capturing complex temporal patterns.

Diffusion models for TSF are commonly formulated as conditional generative models, where the objective is to generate future sequences conditioned on past observations and, optionally, additional contextual information [26, 35, 36, 37]. During training, Gaussian noise is gradually added to the ground-truth future sequence through a forward diffusion process. A neural network guided by the historical context is then trained to reverse this noising process. At inference time, the model generates forecasts by iteratively denoising the noise, effectively sampling from the learned conditional distribution. Compared to conventional models, diffusion-based approaches offer several key advantages: (1) they produce probabilistic forecasts, enabling uncertainty quantification by sampling multiple plausible futures; (2) they exhibit stable training behavior and avoid adversarial instability; and (3) they offer flexible generative capabilities, allowing seamless integration with various conditioning signals such as covariates, control variables, or multimodal inputs. Therefore, it is essential to provide a comprehensive review of the diffusion models for TSF, given that most existing literature reviews of the TSF approaches focus on other approaches [38, 39, 40].

In this paper, we provide a comprehensive survey of diffusion models for TSF. We begin by reviewing the foundation diffusion models, including Denoising Diffusion Probabilistic Model (DDPM) [32], Denoising diffusion implicit model (DDIM) [41], and their extensions incorporating Classifier Guidance [42] and Classifier-Free Guidance [43] (Section 2). We then propose a systematic taxonomy to classify existing diffusion-based TSF approaches along two dimensions: conditioning source (e.g., historical time series and multimodal data) (Section 3), and condition integration process (e.g., feature-centric condition and diffusion-centric condition) (Section 4). For each category, we summarize its common traits and highlight representative approaches. Furthermore, we review widely used datasets (Section 5) and evaluation metrics (Section 6). Finally, we present an overall analysis of existing approaches, highlight their current limitations (Section 7), and propose potential directions for future research (Section 8). Through this survey, we aim to synthesize recent advances, reveal design patterns, and provide insights into the evolving landscape of diffusion-based TSF.

2 Foundation Diffusion Models for TSF

Standard diffusion models define a generative process that progressively adds noise to data through a forward trajectory and reconstructs the original sample via a reverse denoising process. Conditional diffusion models² extend this framework by introducing auxiliary information, such as labels or historical time series, to guide the generation process. A representative diffusion model is DDPM

²Unless otherwise specified, the “*diffusion model*” (as well as its specific version, e.g., DDPM [32]) in the following text stand for the conditional diffusion model.

[32], which achieves high-quality generation but requires many iterative sampling steps, resulting in slow inference speed. DDIM [41] addresses this limitation by reformulating the reverse process as a deterministic trajectory, which accelerates sampling while maintaining compatibility with the original model. In TSF, the objective is to generate future sequences conditioned on past observations, making the task a natural fit for conditional diffusion models. The conditioning input typically consists of historical time series, and the model learns to reconstruct future values from noise under this context. Recent research [44, 45, 46] in diffusion-based TSF also introduces guidance techniques to control the influence of conditioning signals during generation, enabling more flexible and robust forecasting. The following sections provide a detailed roadmap of these concepts, including the mathematical formulation of DDPM and DDIM, the adaptation of conditional diffusion models for TSF, and the integration of guidance mechanisms for enhanced controllability.

2.1 Denoising Diffusion Probabilistic Model (DDPM)

Denoising Diffusion Probabilistic Models (DDPMs) [32] define a generative process by progressively adding and removing noise through a sequence of forward and reverse steps, conditioned on auxiliary information. Let \mathbf{Y}_0 denote the original data sample, and \mathbf{c} the conditioning input. DDPM constructs a forward diffusion process that corrupts \mathbf{Y}_0 into a noise distribution and a reverse process that reconstructs \mathbf{Y}_0 from noise conditioned on \mathbf{c} . The following illustrates the details of the forward diffusion process and the reverse denoising process.

Forward Diffusion Process The forward process corrupts the data \mathbf{Y}_0 using a predefined noise variance schedule $\{\beta_t\}_{t=1}^T$, where β_t is the noise variance at diffusion step t , and T is the total diffusion steps. The entire forward process forms a Markov chain that is formulated by

$$q(\mathbf{Y}_{1:T} | \mathbf{Y}_0) = \prod_{t=1}^T q(\mathbf{Y}_t | \mathbf{Y}_{t-1}) \quad (1)$$

where $q(\cdot | \cdot)$ denotes the forward process distribution and \mathbf{Y}_t is the latent variable at diffusion step t . In addition, $\mathbf{Y}_{1:T}$ is a noisy data sequence from diffusion step 1 to T . Meanwhile, $q(\mathbf{Y}_t | \mathbf{Y}_{t-1}) = \mathcal{N}(\cdot; \boldsymbol{\mu}, \boldsymbol{\Sigma})$ is a multivariate Gaussian distribution with mean $\boldsymbol{\mu} = \sqrt{1 - \beta_t} \mathbf{Y}_{t-1}$ and covariance $\boldsymbol{\Sigma} = \beta_t \mathbf{I}$ (where \mathbf{I} denotes the identity matrix). By simplification, the latent variable \mathbf{Y}_t are sampled from a distribution directly conditioned on \mathbf{Y}_0 :

$$q(\mathbf{Y}_t | \mathbf{Y}_0) = \mathcal{N}(\mathbf{Y}_t; \sqrt{\bar{\alpha}_t} \mathbf{Y}_0, (1 - \bar{\alpha}_t) \mathbf{I}) \quad (2)$$

where $\alpha_t = 1 - \beta_t$ and $\bar{\alpha}_t = \prod_{i=1}^t \alpha_i$. The distribution of the endpoint \mathbf{Y}_T of the forward process obeys a Gaussian distribution $\mathcal{N}(\mathbf{0}, \mathbf{I})$ with mean $\mathbf{0}$ and covariance \mathbf{I} (i.e., $\mathbf{Y}_T \sim \mathcal{N}(\mathbf{0}, \mathbf{I})$).

Reverse Denoising Process Contrary to the forward process, the reverse process reconstructs \mathbf{Y}_{t-1} from \mathbf{Y}_t via a transition distribution $p_\theta(\cdot | \cdot)$ parametrized by θ , which is formulated as

$$p_\theta(\mathbf{Y}_{t-1} | \mathbf{Y}_t, \mathbf{c}) = \mathcal{N}(\mathbf{Y}_{t-1}; \boldsymbol{\mu}_\theta(\mathbf{Y}_t, \mathbf{c}, t), \boldsymbol{\Sigma}_\theta(\mathbf{Y}_t, \mathbf{c}, t)), \quad (3)$$

where $\boldsymbol{\mu}_\theta(\cdot)$ is the parameterized mean function and $\boldsymbol{\Sigma}_\theta(\cdot)$ is the parameterized covariance function. In practice, $\boldsymbol{\Sigma}_\theta(\cdot)$ is often simplified to $\sigma_t^2 \mathbf{I}$ that depends only on t . In training, the model minimizes the KL-divergence between the reverse process $p_\theta(\mathbf{Y}_{t-1} | \mathbf{Y}_t, \mathbf{c})$ and the forward process posterior $q(\mathbf{Y}_{t-1} | \mathbf{Y}_t, \mathbf{Y}_0)$. According to Ho et al. [32], this objective is simplified to a noise prediction loss \mathcal{L} computed by

$$\mathcal{L} = \mathbb{E}_{\mathbf{Y}_0, \mathbf{c}, t, \epsilon} \left[\|\epsilon - \epsilon_\theta(\mathbf{Y}_t, \mathbf{c}, t)\|^2 \right] \quad (4)$$

where $\epsilon \sim \mathcal{N}(\mathbf{0}, \mathbf{I})$ is the Gaussian noise added in the forward process, and $\epsilon_\theta(\cdot)$ is the noise prediction network with conditional \mathbf{c} as input. In addition, $\mathbb{E}[\cdot]$ denotes the expectation operation and $\|\cdot\|^2$ represents Euclidean norm function. During inference, the model iteratively applies the conditional reverse transitions starting from $\mathbf{Y}_T \sim \mathcal{N}(\mathbf{0}, \mathbf{I})$ as

$$\mathbf{Y}_{t-1} \sim p_\theta(\mathbf{Y}_{t-1} | \mathbf{Y}_t, \mathbf{c}), \quad t = T, T-1, \dots, 1. \quad (5)$$

Among them, $\hat{\mathbf{Y}}_0$ sampled at step $t = 1$ is the final result of prediction based on the condition \mathbf{c} .

2.2 Denoising Diffusion Implicit Model (DDIM)

DDPMs require sampling over hundreds to thousands of total diffusion steps to produce high-quality samples, resulting in prolonged inference times. Accelerating this sampling process, denoising diffusion implicit models (DDIMs) [41] reformulate it as a non-Markovian deterministic process. This reformulation permits skipping steps, enabling the attainment of equivalent generation quality using substantially fewer sampling steps than the total diffusion steps. According to Song et al. [41], DDIMs share the identical forward process with DDPMs. Consequently, DDIMs sampling becomes directly applicable to pre-trained DDPMs without requiring retraining. This property provides a practical path for deploying diffusion models efficiently. Specifically, DDIMs reformulates the reverse process as

$$\mathbf{Y}_{t-1} = \sqrt{\bar{\alpha}_{t-1}} \cdot \mathbf{Y}_t + \sqrt{1 - \bar{\alpha}_{t-1}} \cdot \epsilon_\theta(\mathbf{Y}_t, \mathbf{c}, t) \quad (6)$$

where \mathbf{Y}_θ is computed by

$$\mathbf{Y}_\theta = \frac{1}{\sqrt{\bar{\alpha}_t}} \left(\mathbf{Y}_t - \sqrt{1 - \bar{\alpha}_t} \cdot \epsilon_\theta(\mathbf{Y}_t, \mathbf{c}, t) \right) \quad (7)$$

Compared to DDPMs, DDIMs eliminates stochasticity in the reverse process by removing the random noise term at each step, while preserving the marginal distributions of the original diffusion trajectory. The step-skip sampling in DDIMs eliminates the need to iterate over all T time steps in the reverse denoising process. Instead, DDIM samples only on a subset of diffusion steps $t_{s_1}, t_{s_2}, \dots, t_{s_S}$, where $t_{s_1} = T$ and $t_{s_S} = 0$. Specifically, for sampling step k from 1 to $S - 1$, the DDIMs computes $\mathbf{Y}_{t_{s_{k-1}}}$ from $\mathbf{Y}_{t_{s_k}}$ using Eq. (6) and replaces t and $t - 1$ with t_{s_k} and $t_{s_{k-1}}$, respectively.

Beyond DDIMs, several advanced sampling techniques are proposed to accelerate diffusion models. For instance, Analytic-DPM [47] leverages closed-form solutions to the reverse diffusion ordinary differential equation, enabling direct computation of sample trajectories without iterative simulation. DPM-Solver [48] applies high-order numerical solvers to the reverse process, replacing the standard Euler approach with more accurate and efficient integration schemes. These approaches further reduce inference time and improve sample quality by optimizing the reverse trajectory computation.

2.3 Applying Diffusion Models for TSF

A straightforward approach to applying diffusion models to TSF is to set the original data \mathbf{Y}_0 as the future time series $\mathbf{x}_{1:H} = (x_1, x_2, \dots, x_i, \dots, x_H)$, where H is the prediction horizon and x_i denotes the time series value at timestep i . Meanwhile, the condition \mathbf{c} in diffusion model equals to the historical time series $\mathbf{x}_{-L+1:0} = (x_{-L+1}, x_{-L+2}, \dots, x_0)$ with L denoting the length of the history time series. In this formulation, the model learns the conditional distribution $q(\mathbf{x}_{1:H} | \mathbf{x}_{-L+1:0})$ of future values given historical time series $\mathbf{x}_{-L+1:0}$. The forward diffusion process corrupts the future time series $\mathbf{x}_{1:H}$ with Gaussian noise over T steps, while the reverse process reconstructs $\mathbf{x}_{1:H}$ from noise $\mathbf{x}_{1:H}^T \sim \mathcal{N}(\mathbf{0}, \mathbf{I})$, conditioned on the historical time series $\mathbf{x}_{-L+1:0}$. Specifically, the DDPM for TSF, as illustrated in Figure 1, defines the forward process as

$$q(\mathbf{x}_{1:H}^{1:T} | \mathbf{x}_{1:H}^0) = \prod_{t=1}^T q(\mathbf{x}_{1:H}^t | \mathbf{x}_{1:H}^{t-1}) \quad (8)$$

where $\mathbf{x}_{1:H}^t$ is the latent variable at diffusion step t and the forward progress transition is formulated as

$$q(\mathbf{x}_{1:H}^t | \mathbf{x}_{1:H}^{t-1}) = \mathcal{N}(\mathbf{x}_{1:H}^t; \sqrt{1 - \beta_t} \mathbf{x}_{1:H}^{t-1}, \beta_t \mathbf{I}) \quad (9)$$

Meanwhile, the reverse process is parameterized as

$$p_\theta(\mathbf{x}_{1:H}^{t-1} | \mathbf{x}_{1:H}^t, \mathbf{x}_{-L+1:0}) = \mathcal{N}(\mathbf{x}_{1:H}^{t-1}; \boldsymbol{\mu}_\theta(\mathbf{x}_{1:H}^t, \mathbf{x}_{-L+1:0}, t), \Sigma_\theta(\mathbf{x}_{1:H}^t, \mathbf{x}_{-L+1:0}, t)) \quad (10)$$

The training objective is to minimize

$$\mathcal{L} = \mathbb{E}_{\mathbf{x}_{1:H}^0, \mathbf{x}_{-L+1:0}, t, \epsilon} \left[\left\| \epsilon - \epsilon_\theta(\mathbf{x}_{1:H}^t, \mathbf{x}_{-L+1:0}, t) \right\|^2 \right] \quad (11)$$

The DDIM variant for TSF also modifies the reverse process to a deterministic trajectory which is formulated as

$$\mathbf{x}_{1:H}^{t-1} = \sqrt{\bar{\alpha}_{t-1}} \cdot \mathbf{x}_\theta + \sqrt{1 - \bar{\alpha}_{t-1}} \cdot \epsilon_\theta(\mathbf{x}_{1:H}^t, \mathbf{x}_{-L+1:0}, t) \quad (12)$$

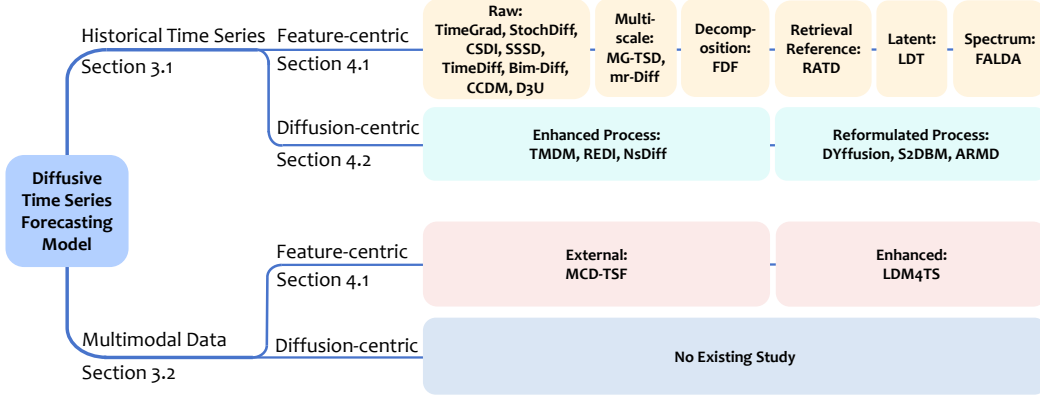


Figure 2: Overview of Diffusion Models for TSF. Each approach is categorized by its conditional source and condition integration process. To the best of our knowledge, there is no study that uses a diffusion-centric model to encode multimodal data for TSF.

where \mathbf{x}_θ is derived from the predicted noise and the conditioning input:

$$\mathbf{x}_\theta = \frac{1}{\sqrt{\bar{\alpha}_t}} \left(\mathbf{x}'_{1:H} - \sqrt{1 - \bar{\alpha}_t} \cdot \epsilon_\theta(\mathbf{x}'_{1:H}, \mathbf{x}_{-L+1:0}, t) \right) \quad (13)$$

In the field of conditional generation for vision, guidance techniques are proposed to flexibly control the strength of conditioning and improve sample quality. Recent studies in diffusion-based TSF also adapt guidance mechanisms to incorporate additional conditioning sources without modifying model architectures. Guidance mechanisms provide a way to steer the generation process toward desired properties or constraints. One of these techniques, named classifier guidance, modifies the reverse process by adding the gradient of a classifier³ $p_{\text{clf}}(\mathbf{x}_{-L+1:0})$ trained to predict the historical time series $\mathbf{x}_{-L+1:0}$ from the noisy future sequence $\mathbf{x}'_{1:H}$. According to Dhariwal and Nichol [42], the guidance is simplified to an update to the mean function:

$$\tilde{\boldsymbol{\mu}}_\theta = \boldsymbol{\mu}_\theta(\mathbf{x}'_{1:H}, \mathbf{x}_{-L+1:0}, t) + s \cdot \nabla_{\mathbf{x}'_{1:H}} \log p_{\text{clf}}(\mathbf{x}_{-L+1:0} | \mathbf{x}'_{1:H}) \quad (14)$$

where $\tilde{\boldsymbol{\mu}}_\theta$ is the updated mean function, ∇ is the gradient operator and s represents guidance scale.

Different from the classifier guidance that requires additional training of a classifier, classifier-free guidance [43] trains the diffusion model to handle both conditional and unconditional generations by randomly dropping the conditioning input during training. At inference, the model combines the conditional and unconditional predictions to update the predicted noise:

$$\epsilon_{\text{guided}} = (1 + s) \cdot \epsilon_\theta(\mathbf{x}'_{1:H}, \mathbf{x}_{-L+1:0}, t) - s \cdot \epsilon_\theta(\mathbf{x}'_{1:H}, \emptyset, t) \quad (15)$$

where $\epsilon_\theta(\mathbf{x}'_{1:H}, \emptyset, t)$ is the unconditional noise prediction and \emptyset represents the historical time series is set to a null tensor. These mechanisms enable flexible integration of historical and auxiliary information in diffusion-based TSF models.

3 Conditions for TSF Diffusion Models

TSF with diffusion models is a conditional generation task; therefore, the design of conditioning information is critical to the forecasting performance. Especially for diffusion-based TSF approaches that use historical data as conditions, how much useful information is extracted from the historical data and the richness of the historical data are critical for the sequence modeling. This characteristic motivates diffusion-based TSF approaches to improve and expand their conditioning source. Therefore, we categorize existing research into two primary groups based on their historical conditioning sources: historical time series conditions and multimodal conditions. For historical time series conditions, we

³Although TSF denotes this component as a predictor, we use the term “classifier” here to remain consistent with the original technique’s nomenclature.

analyze how existing approaches explicitly incorporate specific temporal priors into the condition. This integration guides the sampling process towards generating accurate future time series consistent with underlying temporal patterns. For multimodal conditioning sources, we detail current diffusion-based multimodal time series approaches. These approaches incorporate non-time-series modality information from distinct perspectives, each possessing unique characteristics. The following sections elaborate on these different categories of studies, explaining their methodologies and characteristics.

3.1 Conditioning on Historical Time Series

Generally, the raw historical time series itself directly serves as the condition for diffusion models without requiring additional preprocessing. Most studies in the field utilize this straightforward approach, primarily focusing on improving the architecture of the diffusion model. Beyond using the raw series, applying specific time series processing techniques and transformations enables the extraction and explicit representation of more temporal information, thereby incorporating domain-specific prior knowledge as conditioning signals. For instance, decomposition techniques [49] separate the time series into distinct components, such as trend, seasonality, and residuals. These components capture different aspects of the temporal dynamics, enhancing models' interpretability and simplifying the learning task by isolating underlying patterns. Consequently, approaches such as mr-Diff [50] and FDF [51] decompose the historical time series into trend and seasonal residual terms before diffusion. This decomposition explicitly injects disentangled temporal information as hierarchical conditions into the reverse process. Furthermore, time series inherently possess multi-scale characteristics, where different temporal scales reveal varying degrees of trend evolution and cyclical behavior. MG-TSD [52] and mr-Diff [50] leverage this property by employing representations of the series at multiple scales as conditions during the reverse process. This alignment connects the intermediate diffusion states to different granularity levels, mirroring the coarse-to-fine refinement in time series generation. Beyond these time-domain techniques, frequency-domain transformations convert the time-evolving sequence values into sparse spectral representations. Diffusion-TS [53] and FALDA [54] adopt this strategy, conditioning the diffusion process on both the original historical series and its frequency spectrum. This dual-domain conditioning supplies complementary perspectives on the sequence modeling. Other novel approaches include retrieval augmentation. RATD [55] integrates a mechanism inspired by the natural language processing domain, retrieving the most similar historical sequence segments from the training set as reference time series. Combining these retrieved references with the original time series provides conditions that help the model learn highly repetitive intrinsic temporal patterns effectively. In another direction of these approaches, LDT [46] employs a variational autoencoder to transform the time series into a compressed latent representation before diffusion. This latent space transformation automatically extracts salient features for conditioning while simultaneously reducing computational costs associated with high-dimensional time series.

3.2 Conditioning on Multimodal Data

Beyond preprocessing and transformation techniques that extract useful information from historical time series as domain-specific priors, incorporating multimodal data as additional condition sources provides richer conditioning information. Multimodal approaches [56] gain increasing attention in the TSF domain. Meanwhile, diffusion-based TSF approaches also integrate additional modal information as complementary conditions. For instance, LDM4TS [57] applies complementary vision transformation to convert time series into multi-view images. It also constructs textual descriptions for the time series using predefined templates filled with the statistical features of the time series. These generated images and text descriptions serve as multimodal conditions injected into the reverse process. They guide the diffusion model to predict future time series values based on both visual patterns and semantic text features. Crucially, LDM4TS [57] utilizes only the original time series data itself to create these modalities. This self-contained nature allows straightforward application to existing datasets. Furthermore, the MCD-TSF [58] approach incorporates external news article text recorded concurrently with the target time series. This external text potentially contains information absent from the series data itself. Such external multimodal data offers valuable supplementary conditioning, particularly in forecasting scenarios with frequent external interventions. Conversely, approaches relying on external data impose mandatory external data requirements on time series datasets, which may restrict their applicability across different domains or data availability contexts.

4 Condition Integration

In addition to the source used for conditioning, diffusion-based TSF approaches also differ in *how* they integrate conditioning information into the generative diffusion process. Different from image-to-text or image-to-image generation that focus on transferring features and styles, time series forecasting instead extends historical data into future sequences, so the condition integration mechanism is crucial for ensuring coherent evolution from past to future. Therefore, we classify existing condition integration mechanisms into two primary categories, *feature-centric* and *diffusion-centric* approaches. Feature-centric strategies [35, 59, 60] employ the standard diffusion model. These approaches rely on a well-designed network to extract useful features from the historical conditioning data. These features then guide each denoising step in the reverse diffusion process, ensuring that the generated sequence remains temporally consistent with its historical context. Consequently, the condition acts primarily as input to the learned denoising function. Diffusion-centric approaches [61, 62, 63] propose modifications to the diffusion process. Such techniques incorporate historical data priors directly into both forward and reverse diffusion trajectories, enabling each step to adapt dynamically to past information. By conditioning adjustments on the preceding context, they deliver finer-grained control over the generative process. This dynamic mechanism adapts diffusion dynamics based on the specific temporal features extracted from the historical data. An overview of the diffusion-based TSF approaches and their categorization by conditioning source and integration process is illustrated in Figure 2. The subsequent sections explain these various study categories, detailing their methodologies and characteristics.

4.1 Feature-centric Condition

The feature-centric approaches [35, 59, 60] retain the standard diffusion model’s forward noising and reverse denoising processes. These approaches focus on designing an effective feature extractor that is capable of extracting time-dependent features or modeling time-series uncertainty from historical data, which is formulated as

$$p_{\theta}(\mathbf{x}_{1:H}^{t-1} | \mathbf{x}_{1:H}^t, \mathbf{x}_{-L+1:0}) = \mathcal{N}(\mathbf{x}_{1:H}^{t-1}; \boldsymbol{\mu}_{\theta}(\mathbf{x}_{1:H}^t, t, \phi(\mathbf{x}_{-L+1:0})), \boldsymbol{\Sigma}_{\theta}(\mathbf{x}_{1:H}^t, t, \phi(\mathbf{x}_{-L+1:0}))) \quad (16)$$

where $\phi(\cdot)$ is the feature extractor. To capture the temporal dependencies across consecutive time steps in time-series data, early approaches such as TimeGrad [35] employ a recurrent neural network (RNN) as the model. This RNN processes historical time-series data and performs predictions in an autoregressive manner. Specifically, TimeGrad leverages the RNN-derived hidden state \mathbf{h}_{i-1} at timestep i to guide denoising. The hidden state \mathbf{h}_{i-1} encapsulates historical dynamics through the feature $\mathbf{h}_i = \text{RNN}(\text{concat}(\mathbf{x}_i, \mathbf{c}_i), \mathbf{h}_{i-1})$, where \mathbf{c}_i denotes covariates, and $\text{concat}(\cdot)$ represents concatenation operation. Similarly, StochDiff [59] innovates by integrating the diffusion process into the time series modeling stage, applying diffusion at each time step i within a recurrent framework. The model constructs a data-driven prior $\mathbf{z}_i \sim \mathcal{N}(\boldsymbol{\mu}_{\theta}(\mathbf{h}_{i-1}), \boldsymbol{\Sigma}_{\theta}(\mathbf{h}_{i-1}))$ derived from long short-term memory (LSTM) hidden states \mathbf{h}_{i-1} . The hidden state updates as $\mathbf{h}_i = \text{LSTM}(\text{concat}(\mathbf{x}_i, \mathbf{c}_i), \mathbf{h}_{i-1})$. This prior refines the reverse diffusion as another conditioning feature. While these recursive approaches capture temporal dynamics to some extent, their autoregressive prediction manner leads to error accumulation, consequently resulting in suboptimal long-term forecasting performance. To better capture long-range temporal dependencies, CSDI [60] replaces RNNs with a transformer-based feature extracting network, utilizing self-attention to establish direct interactions between any two time steps. This network conditions on historical time series $\mathbf{x}_{-L+1:0}$ and outputs predicted time series $\hat{\mathbf{x}}_{1:H}$ for all future steps simultaneously, eliminating error accumulation from autoregressive prediction. Building upon these foundation, SSSD [36] reconstructs the feature extracting network using structured state space models (S4) to enhance efficiency. It employs integrates structured S4 as the backbone of its denoise network architecture, specifically targeting the learning of long-range dependencies within sequences while improving inference speed.

In another line of these approaches, TimeDiff [64] proposes two novel conditioning mechanisms, named future mixup and autoregressive initialization, which differ from prior feature-centric approaches. Future mixup creates a conditioning signal \mathbf{z}_{mix} during training by stochastically blending a projection of the history $\mathcal{F}(\mathbf{x}_{-L+1:0})$ with elements of the ground-truth future $\mathbf{x}_{1:H}$ according to a mask \mathbf{m}_t , expressed as

$$\mathbf{z}_{\text{mix}} = \mathbf{m}_t \odot \mathcal{F}(\mathbf{x}_{-L+1:0}) + (\mathbf{1} - \mathbf{m}_t) \odot \mathbf{x}_{1:H} \quad (17)$$

where \odot denotes Hadamard product. Meanwhile, autoregressive initialization produces a simple forecast \mathbf{z}_{ar} from the history using a pretrained linear model defined by

$$\mathbf{z}_{\text{ar}} = \sum_{i=-L+1}^0 \mathbf{W}_i \odot \mathbf{X}_i^0 + \mathbf{B} \quad (18)$$

where \mathbf{X}_i^0 is a matrix formed by replicating the historical value \mathbf{x}_i across H future time steps, and \mathbf{W}_i , \mathbf{B} represent learnable weight and bias parameters. These two components are combined, forming the final condition $\mathbf{c} = \text{concat}(\mathbf{z}_{\text{mix}}, \mathbf{z}_{\text{ar}})$. These mechanisms strengthen temporal dependence modeling by enriching the conditioning signal and reducing disharmony between the observed past and predicted future segments. Building on TimeDiff’s future mixup conditioning mechanism, mr-Diff [50] extends this concept by incorporating multi-scale historical inputs \mathbf{X}_s derived from seasonal-trend decomposition. In addition, Bim-Diff [65] integrates brain-inspired semantic memory \mathbf{m}_s and episodic memory \mathbf{m}_e as variational priors into the conditioning signal. These memories encode cross-channel recurrent patterns through attention mechanisms:

$$\mathbf{m}_s^j = \sum_i \frac{\text{score}(\mathbf{M}_{s,i}, \mathbf{h}_j)}{\sum_i \text{score}(\mathbf{M}_{s,i}, \mathbf{h}_j)} \mathbf{M}_{s,i}, \quad \mathbf{m}_e^j = \sum_i \frac{\text{score}(\mathbf{M}_{e,i}, \mathbf{h}_j)}{\sum_i \text{score}(\mathbf{M}_{e,i}, \mathbf{h}_j)} \mathbf{M}_{e,i} \quad (19)$$

where \mathbf{h}_j represents the query vector for channel j . \mathbf{m}_s^j and \mathbf{m}_e^j denote the semantic memory and episodic memory on the j -th channel, respectively. In addition, \mathbf{M}_s and \mathbf{M}_e are learnable vectors. The combined memory prior $\mathbf{m} = \mathbf{m}_s + \mathbf{m}_e$ enriches the condition as $\mathbf{c}_{\text{mix}} = \mathbf{m}_t \odot \mathbf{W}\mathbf{m} + (\mathbf{1} - \mathbf{m}_t) \odot \mathbf{x}_{1:H}$, where \mathbf{W} projects memories into the condition space. This design explicitly incorporates recurring temporal structures into the diffusion process while maintaining mixup’s boundary harmonization. Similarly, to elaborate on the inter-channel modeling approach, CCDM [66] utilizes a channel-aware feature extracting network combining channel-independent multi-layer perceptron encoders (CiDM) for univariate patterns and channel-mixing diffusion Transformers (DiT) for cross-variate correlations. The architecture integrates d -channel features through:

$$\mathbf{G} = \text{DiT}(\text{concat}(\{\text{CiDM}(\mathbf{x}_{d,-L+1:0})\}_{d=1}^D, \mathbf{x}'_{1:H})) \quad (20)$$

where \mathbf{G} denotes the fused feature tensor and D is the channel number of time series.

A different line of feature-centric approaches is uncertainty modeling by leveraging specialized feature extraction architectures. For example, D3U [67] leverages a pre-trained point forecasting model to extract deterministic features $\hat{\mathbf{y}}_{1:H}$ from historical data $\mathbf{x}_{-L+1:0}$ and computes residuals $\mathbf{r}_{1:H}^0 = \mathbf{y}_{1:H} - \hat{\mathbf{y}}_{1:H}$ as high-uncertainty components. These residuals are modeled by a conditional diffusion process where a patch-based denoising network (PatchDN) $\mathbf{r}_\theta(\mathbf{r}_{1:H}^t, t|\mathbf{c})$ predicts $\mathbf{r}_{1:H}^0$ at diffusion step t using the reverse transition as

$$\mu_\theta(\mathbf{r}_{1:H}^t, t|\mathbf{c}) = \frac{\sqrt{\alpha_t}(1 - \bar{\alpha}_{t-1})}{1 - \bar{\alpha}_t} \mathbf{r}_{1:H}^t + \frac{\sqrt{\bar{\alpha}_{t-1}}\beta_t}{1 - \bar{\alpha}_t} \mathbf{r}_\theta(\mathbf{r}_{1:H}^t, t|\mathbf{c}) \quad (21)$$

PatchDN utilizes patch embeddings and adaptive layer normalization (AdaLN) to incorporate conditional features \mathbf{c} for scale and shift modulation, thereby refining uncertainty estimation. The final prediction combines deterministic output $\hat{\mathbf{y}}_{1:H}$ and sampled residuals $\hat{\mathbf{r}}_{1:H}^0$, yielding $\hat{\mathbf{y}}_{1:H} + \hat{\mathbf{r}}_{1:H}^0$. On top of this work, FALDA [54] incorporates Fourier decomposition to decouple time series into distinct non-stationary, stationary, and noise components. The approach utilizes a lightweight denoise network with moving average decomposition and AdaLN to explicitly isolate aleatoric uncertainty patterns. Different from D3U’s transformer-based patch processing, FALDA [54] conditions on pure historical noise terms and targets direct residual reconstruction, separating epistemic uncertainty through component-specific modeling.

4.2 Diffusion-centric Condition

Diffusion-centric approaches modify the forward process and the reverse process of diffusion models. These approaches follow two primary directions. One research direction integrates time series priors into the forward process, enabling a noise addition procedure specific to time-series data. This prior information also guides learning within the reverse process. The other direction replaces the standard noise addition diffusion with alternative processes, such as a deterministic interpolation process. Such

modifications reduce uncertainty inherent in TSF tasks. Both directions represent adaptations of the core diffusion framework to enhance performance for TSF.

Real-world time series inherently possess time-varying uncertainties due to external physical factors. Standard diffusion models enforce a consistent stationary distribution, namely Gaussian noise $\mathcal{N}(\mathbf{0}, \mathbf{I})$, at the diffusion endpoint for all time series. This motivates recent approaches to incorporate prior knowledge from historical time series within the forward diffusion process. For example, TMDM [61] integrates a Transformer to extract historical features $\hat{\mathbf{y}}_{1:H}$ from $\mathbf{x}_{-L+1:0}$, utilizing this as a conditional prior in both diffusion processes. The modified forward process interpolates between the future time series $\mathbf{x}_{1:H}^0$ and the conditional prior $\hat{\mathbf{y}}_{1:H}$ as

$$\mathbf{x}_{1:H}^t = \sqrt{\alpha_t} \mathbf{x}_{1:H}^0 + (1 - \sqrt{\alpha_t}) \hat{\mathbf{y}}_{1:H} + \sqrt{1 - \alpha_t} \epsilon \quad (22)$$

In TMDM, the endpoint distribution at diffusion step T is $\mathcal{N}(\hat{\mathbf{y}}_{1:H}, \mathbf{I})$. The reverse process employs the prior $\hat{\mathbf{y}}_{1:H}$ in the denoising function $\epsilon_\theta(\cdot)$ and calculate the $\mathbf{X}_{1:H}^{t-1}$:

$$\mathbf{X}_{1:H}^{t-1} = \frac{1}{\sqrt{\alpha_t}} \left(\mathbf{x}_{1:H}^t - (1 - \sqrt{\alpha_t}) \hat{\mathbf{y}}_{1:H} - \sqrt{1 - \alpha_t} \epsilon_\theta(\mathbf{x}_{1:H}^t, \hat{\mathbf{y}}_{1:H}, t) \right) \quad (23)$$

Then, the prior latent variable $\mathbf{x}_{1:H}^{t-1}$ is obtained by

$$\mathbf{x}_{1:H}^{t-1} = \gamma_0 \mathbf{x}_{1:H}^t + \gamma_1 \mathbf{x}_{1:H}^t + \gamma_2 \hat{\mathbf{y}}_{1:H} + \sqrt{\tilde{\beta}_t} \epsilon \quad (24)$$

where $\gamma_0, \gamma_1, \gamma_2$ and $\tilde{\beta}_t$ are parameters that depend only on β_t . This joint conditioning strategy leverages historical dependencies to refine uncertainty estimation in prediction. Building on TMDM, NsDiff [62] further incorporates a historical-dependent variance to model non-stationary uncertainty. The forward process transitions to an endpoint distribution:

$$\mathcal{N}(\mathbf{f}(\mathbf{x}_{-L+1:0}), \mathbf{g}(\mathbf{x}_{-L+1:0})) \quad (25)$$

where $\mathbf{f}(\cdot)$ and $\mathbf{g}(\cdot)$ are the conditional expected mean function and conditional variance function, respectively. The forward process integrates time-varying variances by

$$\mathbf{x}_{1:H}^t = \sqrt{\alpha_t} \mathbf{x}_{1:H}^0 + (1 - \sqrt{\alpha_t}) \mathbf{f}(\mathbf{x}_{-L+1:0}) + \sqrt{(\tilde{\beta}_t - \beta_t) \mathbf{g}(\mathbf{x}_{-L+1:0}) + \tilde{\beta}_t \sigma_{\mathbf{x}_{1:H}}} \epsilon \quad (26)$$

where $\tilde{\beta}_t$ is a parameter that depend only on α_t and $\sigma_{\mathbf{x}_{1:H}}$ is the actual variance. The reverse process conditions denoising on both $\mathbf{f}(\mathbf{x}_{-L+1:0})$ and $\mathbf{g}(\mathbf{x}_{-L+1:0})$ to refine uncertainty estimation. This approach adapts the diffusion trajectory to temporal uncertainty shifts, improving distributional flexibility. Besides modeling uncertainty, another study integrates recurrent fusion of historical priors within the forward diffusion process to enhance the utilization of recent temporal information. REDI [68] implements a recurrent diffusion mechanism where each forward step combines the current noisy future time series value \mathbf{x}_i^t at time step i with the immediate historical value \mathbf{x}_{i-1}^t before noise addition:

$$\mathbf{x}_i^t = \sqrt{\alpha_t} (\mathbf{x}_i^{t-1} \oplus \mathbf{x}_{i-1}^{t-1}) + \sqrt{1 - \alpha_t} \epsilon \quad (27)$$

where \oplus denotes element-wise addition. The corresponding reverse process denoises \mathbf{x}_i^t to \mathbf{x}_i^{t-1} using the denoised prior \mathbf{x}_{i-1}^{t-1} for step-aware conditioning:

$$\mathbf{x}_i^{t-1} = \mu_\theta(\mathbf{x}_i^t, \mathbf{x}_{i-1}^{t-1}, t) + \frac{1 - \bar{\alpha}_{t-1}}{1 - \bar{\alpha}_t} \beta_t \epsilon \quad (28)$$

This recurrent formulation strengthens focus on proximate history to mitigate distribution drift and ensures strict temporal causality by preventing information leakage from future states during generation.

Beyond the aforementioned approaches, another research direction focuses on developing alternative formulations for the forward diffusion process. This alternative formulation specifically captures the inherent characteristics of time series data. For instance, DYffusion [63] leverages the temporal dynamics in the data, directly coupling it with the diffusion steps. Specifically, this approach designs a stochastic temporal interpolator $I(\cdot)$ for the forward process to generate intermediate states between the initial condition \mathbf{x}_0 and the target future point \mathbf{x}_H , formalized as minimizing $\mathbb{E} \left\| I_\phi(\mathbf{x}_0, \mathbf{x}_H, t) - \mathbf{x}_i \right\|^2$

where i is an intermediate timestep. The reverse process employs a forecaster $F(\cdot)$ to predict \mathbf{x}_H from interpolated states, defined as minimizing $\mathbb{E} \|F(\mathbf{x}_i, i) - \mathbf{x}_H\|^2$, which enhances computational efficiency and enables flexible continuous-time sampling trajectories. S2DBM [69] proposes a Brownian Bridge diffusion process to replace the traditional Gaussian diffusion framework. This approach constructs a stochastic bridge between a historical prior $\mathbf{h} = F_p(\mathbf{x}_{-L+1:0})$ and the target future $\mathbf{x}_{1:H}^0$, formalizing the forward process as

$$\mathbf{x}_{1:H}^t = \hat{\alpha}_t \mathbf{x}_{1:H}^0 + (1 - \hat{\alpha}_t) \mathbf{h} + \sqrt{2\hat{\alpha}_t(1 - \hat{\alpha}_t)} \boldsymbol{\epsilon} \quad (29)$$

where $F_p(\cdot)$ denotes the prior predictor and $\hat{\alpha}_t = 1 - t/T$. The reverse process initializes at $\mathbf{x}_{1:H}^T = \mathbf{h}$ and iteratively refines predictions using

$$\mathbf{x}_{1:H}^{t-1} = \kappa_t \mathbf{x}_{1:H}^t + \lambda_t \mathbf{x}_\theta(\mathbf{x}_{1:H}^t, \mathbf{h}, \mathbf{c}, t) + \zeta_t \mathbf{h} + \hat{\sigma}_t \boldsymbol{\epsilon} \quad (30)$$

where $\kappa_t, \lambda_t, \zeta_t$ are analytical coefficients and $\hat{\sigma}_t^2$ controls variance. This architecture integrates historical information as a fixed endpoint to strengthen temporal dependencies and offers configurable noise levels for deterministic or probabilistic forecasting. ARMD [45] reinterprets the diffusion paradigm, treating the future time series $\mathbf{x}_{1:T}^0$ as the initial state and the historical time series $\mathbf{x}_{-T+1:0}$ as the final state⁴. Its forward process employs a sliding interpolation technique to generate intermediate sequences $\mathbf{x}_{1-t:T-t}^t$, defined as

$$\mathbf{x}_{1-t:T-t}^t = \sqrt{\bar{\alpha}_t} \mathbf{x}_{1:T}^0 + \sqrt{1 - \bar{\alpha}_t} S_w(\mathbf{x}_{1:T}^0, t) \quad (31)$$

where α_t decreases with t , $S_w(\cdot)$ is an evolution trend extraction function as

$$S_w(\mathbf{x}_{1:T}^0, t) = \left(\sqrt{\frac{1}{\bar{\alpha}_t}} \mathbf{x}_{1-t:T-t}^t - \mathbf{x}_{1:T}^0 \right) / \sqrt{\frac{1}{\bar{\alpha}_t} - 1} \quad (32)$$

The reverse process starts from $\mathbf{x}_{-T+1:0}^H = S_w(\mathbf{x}_{-T+1:0})$ and predicts $\mathbf{x}_{2-t:T-t+1}^{t-1}$ by

$$\mathbf{x}_{2-t:T-t+1}^{t-1} = \sqrt{\bar{\alpha}_{t-1}} \hat{X}_\theta^0(\mathbf{x}_{1-t:T-t}^t, t) + \sqrt{1 - \bar{\alpha}_{t-1} - \sigma_t^2} \hat{z}_t \quad (33)$$

where $\hat{X}_\theta^0(\cdot)$ is the devolution network and \hat{z}_t is the predicted evolution trend. This formulation inherently embeds the historical information as the generative endpoint, ensuring the reverse trajectory learns a direct mapping from history to future, enhancing temporal dependence learning and facilitating sequence modeling.

5 Datasets

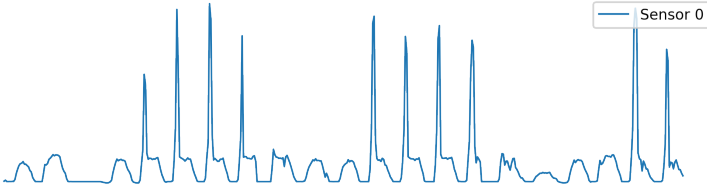
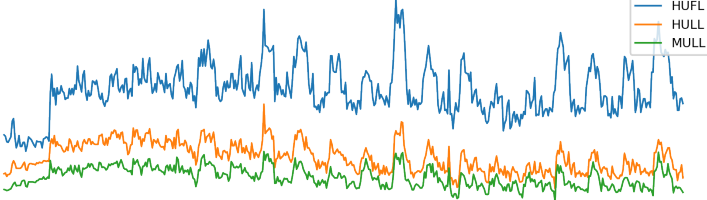
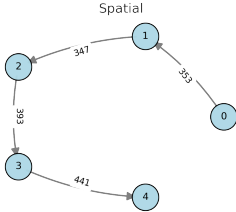
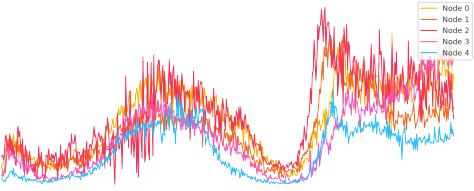
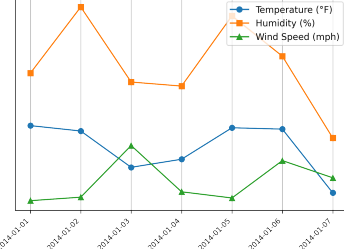
The datasets used for evaluating diffusion-based TSF models are broadly categorized into two types: unimodal time series datasets and multimodal time series datasets. Unimodal time series datasets consist solely of temporal signals, where all available information is encoded in time-indexed numerical sequences. Multimodal datasets integrate time series with other modalities such as text, images, or metadata, enabling richer contextual modeling. Table 1 illustrates representative examples of the four major types of time series data. Table 2 summarizes the benchmark datasets and evaluation metrics used in each diffusion-based TSF approach.

5.1 Unimodal Time Series Datasets

Unimodal time series datasets refer to those where the input consists of purely temporal numerical data, without involving additional modalities such as text or images. These datasets are further categorized into univariate, multivariate, and spatio-temporal types. Univariate sequences track the evolution of a single variable over time, while multivariate ones involve multiple variables with temporal and cross-variable dependencies. In practice, most datasets are inherently multivariate, and univariate sequences are often constructed by selecting a single variable from them. Spatio-temporal sequences further capture both temporal dynamics and spatial dependencies across locations. We summarize several commonly used unimodal time series datasets below.

⁴In ARMD, the length of the history window and the horizon are the same and equal to the diffusion step length, that is, $L = H = T$.

Table 1: Examples of datasets across different time series types.

Type	Datasets	Example
Univariate	Traffic	
Multivariate	ETTh1	
Spatio-temporal	PEMS04	<div style="display: flex; justify-content: space-around;"> <div style="text-align: center;"> <p>Spatial</p>  </div> <div style="text-align: center;"> <p>Temporal</p>  </div> </div>
Multimodal	TTC	 <div style="margin-left: 20px;"> <p>2014-01-01: Arctic air is expected to invade the upp...</p> <p>2014-01-02: Frigid air will sweep into the Midwest, ...</p> <p>2014-01-03: Another arctic plunge is expected for th...</p> <p>2014-01-04: 20°F-40°F below normal temperatures are ...</p> <p>2014-01-05: Temperatures are expected to approach no...</p> <p>2014-01-06: Overview of upper pattern transition fro...</p> <p>2014-01-07: The medium range forecast shows a rebuil...</p> </div>

5.1.1 Univariate and Multivariate

Exchange Rates [70]: A daily multivariate dataset consisting of the exchange rates of 8 foreign currencies relative to USD. It captures long-term trends and cross-currency correlations, making it suitable for financial forecasting.

Weather⁵: A multivariate dataset collected from 21 weather stations in Germany, containing hourly meteorological variables such as temperature, humidity, and wind speed. It is widely used for evaluating long-range forecasting models.

Electricity⁶: A multivariate dataset recording the hourly electricity consumption of 370 clients. Due to its regular seasonality and correlation across variables, it serves as a benchmark for probabilistic and multistep forecasting.

Traffic⁷: A multivariate dataset from the Caltrans Performance Measurement System (PeMS), containing 10-minute interval occupancy rates from 963 traffic sensors in California. It exhibits strong daily patterns and is often used for modeling temporal dependencies across spatial sensors.

Solar Energy⁸: A multivariate dataset consisting of hourly photovoltaic power production data from 137 solar plants in Alabama. It presents regular day-night cycles and weather-induced variability.

⁵<https://www.bgc-jena.mpg.de/wetter/>

⁶<https://archive.ics.uci.edu/ml/datasets/ElectricityLoadDiagrams20112014>

⁷<https://pems.dot.ca.gov/>

⁸<https://www.nrel.gov/grid/solar-power-data.html>

Table 2: Summary of benchmark TSF datasets and evaluation metrics employed in diffusion models.

Approaches	Datasets	Evaluation Metrics
TimeGrad [35]	Exchange, Solar, Electricity, Traffic, Taxi, Wikipedia	CRPS
CSDI [60]	Solar, Electricity, Traffic, Taxi, Wiki	CRPS
SSSD [36]	PTB-XL, Electricity, ETTm1	MSE, MAE, RMSE, MRE
DYffusion [63]	SST, Navier-Stokes	CRPS, MSE, SSR, Time
TimeDiff [64]	NorPool, Caiso, Weather, ETTm1, Wind, Traffic, Electricity, ETTh1, Exchange	MSE, Time
MG-TSD [52]	Solar, Electricity, Traffic, KDD-cup, Taxi, Wikipedia	CRPS, NMAE, NRMSE
TMDM [61]	Exchange, ILI, ETTm2, Electricity, Traffic, Weather	MAE, MSE
mr-Diff [50]	NorPool, Caiso, Traffic, Electricity, Weather, Exchange, ETTh1, ETTm1, Wind	MAE
LDT [46]	Solar, Electricity, Traffic, Taxi, Wikipedia	CRPS, MSE
StochDiff [59]	Exchange, Weather, Electricity, Solar, ECoChG, MMG	NRMSE, CRPS
Bim-Diff [65]	NorPool, Caiso, Electricity, Weather, Exchange, ETTh1, ETTm1, Wind	MAE
CCDM [66]	ETTh1, Exchange, Weather, Appliance, Electricity, Traffic	MSE, CRPS
FDF [51]	ETTh1, ETTh2, ETTm1, ETTm2, Electricity, Exchange, Weather, Wind	MSE, MAE
REDI [68]	Weather, Exchange, M4-Yearly, M4-Quarterly, M4-Monthly	MAE, RMSE
RATD [55]	Exchange, Wind, Electricity, Weather	MSE, MAE, CRPS
S2DBM [69]	ETTh1, ETTh2, ETTm1, ETTm2, ILI, Weather, Exchange	MSE, MAE
ARMD [45]	Metric, Solar, Energy, ETTh1, ETTh2, ETTm1, ETTm2, Exchange, Stock	MSE, MAE
D3U [67]	ETTh1, ETTm2, Weather, Solar-Energy, Electricity, Traffic	MSE, MAE
LDM4TS [57]	ETTh1, ETTh2, ETTm1, ETTm2, Weather, ECL, Traffic	MSE, MAE
MCD-TSF [58]	Time-MMD (Agr, Cli, Eco, Ene, Env, Hea, Soc, Tra)	MSE, MAE
NsDiff [62]	ETTh1, ETTh2, ETTm1, ETTm2, ECL, EXG, ILI, Solar, Traffic	CRPS, QICE
FALDA [54]	ILI, Exchange, ETTm2, Weather, Electricity, Traffic	CRPS

ILI (Influenza-Like Illness)⁹: A univariate weekly dataset of U.S. outpatient visits due to influenza-like illness, published by the CDC. It is widely used for epidemic forecasting and seasonal modeling.

ETT (Electricity Transformer Temperature) [71]: A multivariate dataset capturing the hourly oil temperature of electricity transformers and related external features (e.g., load, ambient temperature). It contains multiple variants (ETTh1, ETTh2, ETTm1, ETTm2) differing in frequency and span.

M3 (Makridakis Competition 3) [72]: A benchmark collection of 3,003 univariate time series from the third Makridakis forecasting competition (M3), covering yearly, quarterly, monthly, and other frequencies across domains such as finance, economics, and industry. It remains widely used for evaluating univariate forecasting accuracy and generalization ability.

5.1.2 Spatio-temporal Datasets

PEMS04 and PEMS08 [73]: Collected by CalTrans via the Performance Measurement System (PEMS) [74], these traffic datasets record 5-minute interval flow and speed data from loop detectors. PEMS04 contains readings from 307 sensors in California District 04 (Jan–Feb 2018), while PEMS08

⁹<https://gis.cdc.gov/grasp/fluview/fluportaldashboard.html>

Table 3: Performance comparison of five approaches on four datasets with a history length of 168 and averaged prediction length results.

Method	Exchange			Wind			Electricity			Weather		
	MSE	MAE	CRPS	MSE	MAE	CRPS	MSE	MAE	CRPS	MSE	MAE	CRPS
RATD	0.013	0.073	0.339	0.784	0.579	0.673	0.151	0.246	0.373	0.281	0.293	0.301
TimeDiff	0.018	0.091	0.589	0.896	0.687	0.917	0.193	0.305	0.490	0.327	0.312	0.410
CSDI	0.077	0.194	0.397	1.066	0.741	0.941	0.379	0.579	0.480	0.356	0.374	0.354
mr-Diff	0.016	0.082	0.397	0.881	0.675	0.881	0.173	0.258	0.429	0.296	0.324	0.347

Table 4: Performance comparison of five approaches on six datasets with a history length of 96 and a prediction length of 192.

Method	ILI		Exchange		Electricity		Traffic		ETTm2		Weather	
	MSE	MAE	MSE	MAE	MSE	MAE	MSE	MAE	MSE	MAE	MSE	MAE
TimeGrad	2.644	1.142	2.429	0.902	0.645	0.723	0.932	0.807	1.385	0.732	0.885	0.551
CSDI	2.538	1.208	1.662	0.748	0.553	0.795	0.921	0.678	1.291	0.576	0.842	0.523
SSSD	2.521	1.079	0.897	0.861	0.481	0.607	0.794	0.498	0.973	0.559	0.693	0.501
TimeDiff	2.458	1.085	0.475	0.429	0.730	0.690	1.465	0.851	0.284	0.342	0.277	0.331
TMDM	1.985	0.846	0.260	0.365	0.222	0.329	0.721	0.411	0.524	0.493	0.244	0.286
D3U	2.103	0.935	0.254	0.358	0.179	0.267	0.468	0.299	0.241	0.302	0.222	0.264
FALDA	1.666	0.821	0.165	0.296	0.163	0.248	0.412	0.251	0.246	0.301	0.215	0.255

includes data from 170 sensors in District 08 (July–Aug 2018).

Sea Surface Temperature (SST)¹⁰ [75]: A daily-resolution global sea surface temperature dataset from NOAA OISSTv2.

Navier–Stokes Flow [76]: A synthetic fluid dynamics dataset simulating incompressible 2D flows on a 221×42 grid. Each instance includes randomly placed circular obstacles, with x/y velocity fields and pressure channels. It serves as a controlled benchmark for physical simulation and partial differential equation (PDE) forecasting.

Spring Mesh [76]: A synthetic physics dataset consisting of a 10×10 particle grid connected by springs. Each node has two positional and two momentum channels. The system evolves based on spring dynamics and provides a clean testbed for structure-aware sequence modeling.

5.2 Multimodal Datasets

Time-MMD (Multi-Domain Multimodal Dataset) [77]: The first large-scale multimodal time series dataset spanning nine diverse domains (e.g., agriculture, climate, economy, energy, health, traffic). Each sample includes aligned numerical time series and fine-grained textual context.

TTC (Time-Text Corpus) [78]: A benchmark comprising temporally aligned pairs of numerical time series and descriptive text in healthcare and climate science.

TimeCAP (Time-Series Contextualization and Prediction) [79]: A framework where large language models serve as both contextualizers and predictors. The dataset includes real-world time series across domains (e.g., weather in New York, finance, healthcare test-positive rates), paired with generated summaries by GPT-4 and labeled event outcomes.

Image-EEG [80]: A large-scale multimodal dataset that pairs time-resolved EEG signals with visual stimuli for human object recognition. It includes brain responses from 10 participants viewing over 22,000 images across 30 object categories.

6 Evaluation Metrics

The performance of a TSF system is evaluated from two complementary perspectives, namely, deterministic metrics and probabilistic metrics. Deterministic metrics compare a single point forecast to the observed value, while probabilistic metrics judge an entire predictive distribution. Tables 3 4 5 present the performance of several diffusion-based TSF methods on multiple benchmark datasets. In the following, we introduce and explain several commonly used evaluation metrics.

¹⁰<https://www.psl.noaa.gov/data/gridded/data.noaa.oisst.v2.highres.html>

Table 5: Performance comparison of six approaches on four datasets, where history and prediction window sizes are individually set: Exchange (90, 7), Weather (144, 144), Electricity (168, 24), and Solar (288, 144).

Method	Exchange		Weather		Electricity		Solar	
	NRMSE	CRPS	NRMSE	CRPS	NRMSE	CRPS	NRMSE	CRPS
TimeGrad	0.066	0.010	0.691	0.527	0.043	0.024	0.973	0.416
SSSD	0.065	0.010	0.755	0.701	0.094	0.065	1.058	0.506
TimeDiff	0.074	0.012	0.702	0.635	0.045	0.036	0.882	0.423
TMDM	0.063	0.010	0.564	0.618	0.063	0.042	0.829	0.382
MG-TSD	0.075	0.009	0.696	0.596	0.032	0.019	0.756	0.375
StochDiff	0.052	0.008	0.491	0.521	0.048	0.029	0.812	0.391

6.1 Deterministic Metrics

Deterministic metrics assess forecasting performance by computing point-wise errors between predicted and ground-truth values. Among them, Mean Squared Error (MSE) and its variants are widely used due to their sensitivity to large deviations and compatibility with gradient-based learning. Similarly, Mean Absolute Error (MAE) offers robust alternatives that are less affected by outliers and better suited for evaluating across different scales. These metrics provide intuitive and interpretable scores, making them a standard choice for deterministic time series forecasting. In the following, we provide detailed definitions and explanations of each metric.

Mean Squared Error (MSE) is computed by

$$\text{MSE} = \frac{1}{H} \sum_{t=1}^H \|x_t - \hat{x}_t\|^2 \quad (34)$$

where x_t denotes the ground-truth value at time t , and \hat{x}_t represents the corresponding forecasted value. While MSE is easy to compute and differentiable, it penalises large deviations quadratically and is therefore sensitive to outliers.

Root Mean Squared Error (RMSE) is computed by

$$\text{RMSE} = \sqrt{\text{MSE}} \quad (35)$$

and it is expressed in the same physical units as the observations, making it easier to interpret than MSE.

Normalized Root Mean Squared Error (NRMSE) is computed by

$$\text{NRMSE} = \frac{\text{RMSE}}{\sqrt{\frac{1}{H} \sum_{t=1}^H \|x_t\|^2}} \quad (36)$$

and it normalizes RMSE by the energy of the true values, yielding a unitless score. It facilitates fair comparison between models or datasets with different scales.

Mean Absolute Error (MAE) is computed by

$$\text{MAE} = \frac{1}{H} \sum_{t=1}^H \|x_t - \hat{x}_t\|_1 \quad (37)$$

where ℓ_1 -norm yields a piece-wise linear loss that is more robust to MSE.

Normalized Mean Absolute Error (NMAE) is computed by

$$\text{NMAE} = \frac{\text{MAE}}{\sum_{t=1}^H \|x_t\|_1} \quad (38)$$

It normalizes the absolute error by the magnitude of the ground-truth values, making the metric unitless and scale-invariant. It is especially useful when comparing performance across datasets or tasks with different value ranges.

6.2 Probabilistic Metrics

While deterministic metrics overlook uncertainty in predictions, probabilistic metrics assess how well the predicted distribution aligns with the actual observed values.

Continuous Ranked Probability Score (CRPS) is computed by

$$\text{CRPS}(F, x) = \int_{-\infty}^{\infty} (F(z) - \mathbb{1}\{x \leq z\})^2 dz \quad (39)$$

Here, $\mathbb{1}\{x \leq z\}$ is the indicator function, which equals 1 if $x \leq z$ and 0 otherwise. It represents the ground-truth step function centered at x . CRPS measures the squared distance between the predicted cumulative distribution function $F(z)$ and the Heaviside step function centered at the ground-truth value x . It generalizes MAE to probabilistic forecasts and reduces to MAE when the predicted distribution collapses to a point estimate. In practice, F is approximated by an empirical cumulative distribution function \hat{F}_N , constructed from an ensemble of N sampled predictions $\{\hat{x}^{(n)}\}_{n=1}^N$.

Normalized Average CRPS (NACRPS) To score an H -step, d -dimensional forecast, NACRPS aggregates the point-wise CRPS values and normalizes them by the total magnitude of the target window:

$$\text{NACRPS} = \frac{\sum_{i=1}^d \sum_{t=1}^H \text{CRPS}(\hat{F}_{i,t}, x_{i,t})}{\sum_{i=1}^d \sum_{t=1}^H |x_{i,t}|}, \quad (40)$$

The $\hat{F}_{i,t}$ denotes the empirical cumulative distribution function (CDF) for variable i at horizon t , constructed from the ensemble of sampled forecasts. The normalization term rescales the score so that variables with larger magnitudes do not dominate the average, thereby enabling fair comparison across heterogeneous datasets.

7 Discussions

In the aforementioned sections, we review the foundation diffusion models and diffusion-based TSF approaches, and then provide a systematic categorization and detailed description of these approaches, focusing on their conditioning sources and integration process. In this section, we summarize key characteristics of current work and discuss the main challenges and limitations that remain in diffusion-based TSF.

7.1 Overall Analysis of Existing Studies

Different from conditional image generation, where diffusion models primarily perform semantic feature transfer, diffusion-based TSF requires learning a temporal transformation from historical observations to future horizons. This fundamental difference introduces unique modeling challenges, prompting researchers to adapt the diffusion process to the temporal dynamics and data structure of time series. Many studies introduce domain-specific priors into the conditioning process. Preprocessing techniques such as trend-seasonality decomposition, multi-scale analysis, and frequency-domain transformations (e.g., Fourier decomposition) are widely adopted to disentangle structured components from the raw historical sequence. These extracted components, such as long-term trends, periodic cycles, and residuals, are incorporated into the diffusion model as structured conditioning inputs. This approach not only improves interpretability but also enhances the model’s ability to generate high-quality forecasts across different temporal scales and frequency bands. Another major direction incorporates multimodal conditioning. Compared with pure time series inputs, auxiliary modalities such as text or images offer additional semantic or contextual signals. For example, visual representations or textual descriptions aligned with temporal data guide the generation process toward more coherent or interpretable outputs. However, successful integration typically requires that these modalities are temporally synchronized and semantically relevant to the target series, which limits their general applicability in domains lacking such aligned data. In addition to enriching the conditioning source, several approaches focus on enhancing the way conditioning is integrated into the

generative process. Rather than relying solely on static context vectors, recent approaches dynamically incorporate historical information through mechanisms such as adaptive noise scheduling, conditional priors embedded into the forward diffusion process, and reinterpreted diffusion trajectories that better reflect temporal causality. These designs seek to exploit the inherently sequential nature of both time series data and the diffusion process, enabling more controllable and temporally aligned generation. In summary, diffusion models hold great promise for TSF, and recent studies have made substantial progress in adapting them to temporal prediction tasks. These adaptations, including the use of temporal priors, multimodal conditioning, and customized integration mechanisms, reflect the increasing maturity of this research direction. Nevertheless, despite these advancements, diffusion-based TSF still faces a number of unresolved limitations and practical challenges.

7.2 Limitations of Current Research

The limitations mainly stem from three aspects. Firstly, TSF itself is inherently challenging. Secondly, diffusion models also come with certain natural limitations. Thirdly, there remains a lack of standardized evaluation protocols in the field.

Limitations from the Nature of TSF TSF inherently presents several challenges that complicate the design of diffusion models. First, real-world time series often exhibit non-stationarity and abrupt regime shifts, making it difficult for models trained under stationary assumptions to generalize across varying temporal dynamics. Second, capturing long-term dependencies remains a fundamental obstacle, as the influence of distant past events may decay or interact in complex, nonlinear ways. Third, data sparsity and irregular sampling are common in practical settings such as healthcare or finance, where missing values and uneven time intervals severely hinder model performance. Lastly, multivariate time series often involve high-dimensional, heterogeneous variables with diverse temporal behaviors and interdependencies, posing significant challenges for stable joint modeling and representation learning.

Limitations of Current Diffusion Models Current diffusion models for TSF also face several limitations. First, the iterative nature of the sampling process often leads to slow inference, requiring a large number of denoising steps to generate each forecast, which restricts their use in real-time applications. Second, most models rely solely on historical time series as the conditioning input, overlooking the potential benefits of incorporating richer modalities such as textual descriptions, spatial context, or external knowledge, which could enhance flexibility and generalization. Third, despite recent efforts [53, 51] to introduce interpretable components like trend or noise decomposition, the generation process remains largely opaque due to the use of high-dimensional latent spaces, limiting the interpretability of predictions. Finally, many existing models are tailored to fixed task settings and struggle to generalize across forecasting horizons, domains, or data distributions, indicating a lack of robustness and transferability in more realistic or zero-shot scenarios.

Lack of Standardized Evaluation Protocols A notable limitation in current diffusion-based TSF research lies in the lack of standardized evaluation protocols. First, datasets are often directly sourced from public repositories and identified only by task-centric names such as “Traffic” or “Electricity”, without clear documentation of data preprocessing steps, variable selections, or temporal resolutions. This ambiguity hinders reproducibility and fair comparison. Second, there is substantial inconsistency in experimental setups across studies, particularly in the choice of historical window length and prediction horizon. These choices are often manually tuned per dataset or model, making cross-method comparisons difficult and potentially biased. Third, the field still lacks a unified benchmarking framework. Existing works adopt diverse metrics, evaluation pipelines, and test splits, which prevents a comprehensive and transparent comparison across approaches. Developing a standardized, modular evaluation benchmark remains an urgent need for future progress.

8 Future Directions

Despite recent advances, diffusion-based TSF continues to face open challenges related to generalization, adaptability, and scalability. These issues suggest several promising avenues for future research, outlined below.

Foundation Models One important direction involves the development of general-purpose time series foundation models that can operate across diverse application domains. Such models are expected to integrate self-supervised pretraining and retrieval-augmented memory, enabling robust few-shot and zero-shot generalization. By learning unified latent representations that align numerical sequences, textual descriptions, and spatial context, these models significantly reduce dependence on domain-specific labels and manual adaptation.

Adaptive Architectures Another promising direction is the design of adaptive model architectures that automatically adjust key forecasting parameters, such as the historical context length and the prediction horizon, based on the characteristics of the input. This adaptability allows a single model to generalize across various forecasting settings without retraining. Potential solutions include hierarchical attention mechanisms, context-aware gating, and inference-time scheduling strategies.

Long-term Multivariate Forecasting Forecasting over extended horizons in high-dimensional multivariate settings remains a major technical challenge. Future models should incorporate explicit mechanisms to mitigate error accumulation. In addition, it is necessary to design efficient architectures that can effectively capture cross-variable dependencies with reduced computational cost. Another promising approach is the incorporation of auxiliary multimodal priors, including textual reports, spatial data, or remote sensing imagery. These complementary information sources enhance forecast stability, interpretability, and robustness in complex real-world domains such as energy management, climate prediction, and financial risk analysis.

References

- [1] Tao Hong and Shu Fan. Probabilistic electric load forecasting: A tutorial review. International Journal of Forecasting, 32(3):914–938, 2016.
- [2] Jui-Sheng Chou and Duc-Son Tran. Forecasting energy consumption time series using machine learning techniques based on usage patterns of residential householders. Energy, 165:709–726, 2018.
- [3] Qiang Wang, Shuyu Li, and Rongrong Li. Forecasting energy demand in china and india: Using single-linear, hybrid-linear, and non-linear time series forecast techniques. Energy, 161: 821–831, 2018.
- [4] Marco Lippi, Matteo Bertini, and Paolo Frasconi. Short-term traffic flow forecasting: An experimental comparison of time-series analysis and supervised learning. IEEE Transactions on Intelligent Transportation Systems, 14(2):871–882, 2013.
- [5] Yaguang Li, Rose Yu, Cyrus Shahabi, and Yan Liu. Diffusion convolutional recurrent neural network: Data-driven traffic forecasting. arXiv preprint arXiv:1707.01926, 2017.
- [6] Jianhu Zheng and Mingfang Huang. Traffic flow forecast through time series analysis based on deep learning. IEEE access, 8:82562–82570, 2020.
- [7] Mustafa Gul and F Necati Catbas. Statistical pattern recognition for structural health monitoring using time series modeling: Theory and experimental verifications. Mechanical Systems and Signal Processing, 23(7):2192–2204, 2009.
- [8] Spilios D Fassois and John S Sakellariou. Statistical time series methods for structural health monitoring. Encyclopedia of structural health monitoring, pages 443–472, 2009.
- [9] Qingnan Sun, Marko V Jankovic, Lia Bally, and Stavroula G Mougiakakou. Predicting blood glucose with an lstm and bi-lstm based deep neural network. In 2018 14th symposium on neural networks and applications (NEUREL), pages 1–5. IEEE, 2018.
- [10] George EP Box, Gwilym M Jenkins, Gregory C Reinsel, and Greta M Ljung. Time series analysis: forecasting and control. John Wiley & Sons, 2015.
- [11] Robert H Shumway, David S Stoffer, Robert H Shumway, and David S Stoffer. Arima models. Time series analysis and its applications: with R examples, pages 75–163, 2017.

- [12] Everette S Gardner Jr. Exponential smoothing: The state of the art. Journal of forecasting, 4(1): 1–28, 1985.
- [13] Rob Hyndman, Anne B Koehler, J Keith Ord, and Ralph D Snyder. Forecasting with exponential smoothing: the state space approach. Springer Science & Business Media, 2008.
- [14] Alysha M De Livera, Rob J Hyndman, and Ralph D Snyder. Forecasting time series with complex seasonal patterns using exponential smoothing. Journal of the American statistical association, 106(496):1513–1527, 2011.
- [15] Jerome T Connor, R Douglas Martin, and Les E Atlas. Recurrent neural networks and robust time series prediction. IEEE transactions on neural networks, 5(2):240–254, 1994.
- [16] Alper Tokgöz and Gözde Ünal. A rnn based time series approach for forecasting turkish electricity load. In 2018 26th Signal processing and communications applications conference (SIU), pages 1–4. IEEE, 2018.
- [17] Hansika Hewamalage, Christoph Bergmeir, and Kasun Bandara. Recurrent neural networks for time series forecasting: Current status and future directions. International Journal of Forecasting, 37(1):388–427, 2021.
- [18] Anastasia Borovykh, Sander Bohte, and Cornelis W Oosterlee. Conditional time series forecasting with convolutional neural networks. arXiv preprint arXiv:1703.04691, 2017.
- [19] Ioannis E Livieris, Emmanuel Pintelas, and Panagiotis Pintelas. A cnn–lstm model for gold price time-series forecasting. Neural computing and applications, 32(23):17351–17360, 2020.
- [20] Sidra Mehtab and Jaydip Sen. Analysis and forecasting of financial time series using cnn and lstm-based deep learning models. In Advances in Distributed Computing and Machine Learning: Proceedings of ICADCML 2021, pages 405–423. Springer, 2022.
- [21] Shiyang Li, Xiaoyong Jin, Yao Xuan, Xiyou Zhou, Wenhu Chen, Yu-Xiang Wang, and Xifeng Yan. Enhancing the locality and breaking the memory bottleneck of transformer on time series forecasting. Advances in neural information processing systems, 32, 2019.
- [22] Neo Wu, Bradley Green, Xue Ben, and Shawn O’Banion. Deep transformer models for time series forecasting: The influenza prevalence case. arXiv preprint arXiv:2001.08317, 2020.
- [23] Haixu Wu, Jiehui Xu, Jianmin Wang, and Mingsheng Long. Autoformer: Decomposition transformers with auto-correlation for long-term series forecasting. Advances in neural information processing systems, 34:22419–22430, 2021.
- [24] Diederik P Kingma, Max Welling, et al. Auto-encoding variational bayes, 2013.
- [25] Danilo Jimenez Rezende, Shakir Mohamed, and Daan Wierstra. Stochastic backpropagation and approximate inference in deep generative models. In International conference on machine learning, pages 1278–1286. PMLR, 2014.
- [26] Yan Li, Xinjiang Lu, Yaqing Wang, and Dejing Dou. Generative time series forecasting with diffusion, denoise, and disentanglement. Advances in Neural Information Processing Systems, 35:23009–23022, 2022.
- [27] Ian J Goodfellow, Jean Pouget-Abadie, Mehdi Mirza, Bing Xu, David Warde-Farley, Sherjil Ozair, Aaron Courville, and Yoshua Bengio. Generative adversarial nets. Advances in neural information processing systems, 27, 2014.
- [28] Alec Radford, Luke Metz, and Soumith Chintala. Unsupervised representation learning with deep convolutional generative adversarial networks. arXiv preprint arXiv:1511.06434, 2015.
- [29] Alireza Koochali, Andreas Dengel, and Sheraz Ahmed. If you like it, gan it—probabilistic multivariate times series forecast with gan. Engineering proceedings, 5(1):40, 2021.
- [30] Jascha Sohl-Dickstein, Eric Weiss, Niru Maheswaranathan, and Surya Ganguli. Deep unsupervised learning using nonequilibrium thermodynamics. In International conference on machine learning, pages 2256–2265. pmlr, 2015.

- [31] Yang Song and Stefano Ermon. Generative modeling by estimating gradients of the data distribution. Advances in neural information processing systems, 32, 2019.
- [32] Jonathan Ho, Ajay Jain, and Pieter Abbeel. Denoising diffusion probabilistic models. Advances in neural information processing systems, 33:6840–6851, 2020.
- [33] Yang Song, Jascha Sohl-Dickstein, Diederik P Kingma, Abhishek Kumar, Stefano Ermon, and Ben Poole. Score-based generative modeling through stochastic differential equations. arXiv preprint arXiv:2011.13456, 2020.
- [34] Yuanhe Tian, Fei Xia, and Yan Song. Diffusion networks with task-specific noise control for radiology report generation. In Proceedings of the 32nd ACM International Conference on Multimedia, pages 1771–1780, 2024.
- [35] Kashif Rasul, Calvin Seward, Ingmar Schuster, and Roland Vollgraf. Autoregressive denoising diffusion models for multivariate probabilistic time series forecasting. In International conference on machine learning, pages 8857–8868. PMLR, 2021.
- [36] Juan Miguel Lopez Alcaraz and Nils Strodthoff. Diffusion-based time series imputation and forecasting with structured state space models. arXiv preprint arXiv:2208.09399, 2022.
- [37] Yuanhe Tian, Chang Liu, Yan Song, Fei Xia, and Yongdong Zhang. Aspect-based sentiment analysis with context denoising. In Findings of the Association for Computational Linguistics: NAACL 2024, pages 3083–3095, 2024.
- [38] Jingjing Xu, Caesar Wu, Yuan-Fang Li, Gregoire Danoy, and Pascal Bouvry. Survey and taxonomy: The role of data-centric ai in transformer-based time series forecasting. arXiv preprint arXiv:2407.19784, 2024.
- [39] Flavio Corradini, Flavio Gerosa, Marco Gori, Carlo Lucheroni, Marco Piangerelli, and Martina Zannotti. A systematic literature review of spatio-temporal graph neural network models for time series forecasting and classification. arXiv preprint arXiv:2410.22377, 2024.
- [40] Habib Irani and Vangelis Metsis. Positional encoding in transformer-based time series models: a survey. arXiv preprint arXiv:2502.12370, 2025.
- [41] Jiaming Song, Chenlin Meng, and Stefano Ermon. Denoising diffusion implicit models. arXiv preprint arXiv:2010.02502, 2020.
- [42] Prafulla Dhariwal and Alexander Nichol. Diffusion models beat gans on image synthesis. Advances in neural information processing systems, 34:8780–8794, 2021.
- [43] Jonathan Ho and Tim Salimans. Classifier-free diffusion guidance. arXiv preprint arXiv:2207.12598, 2022.
- [44] Marcel Kollovich, Abdul Fatir Ansari, Michael Bohlke-Schneider, Jasper Zschiegner, Hao Wang, and Yuyang Bernie Wang. Predict, refine, synthesize: Self-guiding diffusion models for probabilistic time series forecasting. Advances in Neural Information Processing Systems, 36: 28341–28364, 2023.
- [45] Jiabin Gao, Qinglong Cao, and Yuntian Chen. Auto-regressive moving diffusion models for time series forecasting. In Proceedings of the AAAI Conference on Artificial Intelligence, volume 39, pages 16727–16735, 2025.
- [46] Shibo Feng, Chunyan Miao, Zhong Zhang, and Peilin Zhao. Latent diffusion transformer for probabilistic time series forecasting. In Proceedings of the AAAI Conference on Artificial Intelligence, volume 38, pages 11979–11987, 2024.
- [47] Fan Bao, Chongxuan Li, Jun Zhu, and Bo Zhang. Analytic-dpm: an analytic estimate of the optimal reverse variance in diffusion probabilistic models. arXiv preprint arXiv:2201.06503, 2022.
- [48] Cheng Lu, Yuhao Zhou, Fan Bao, Jianfei Chen, Chongxuan Li, and Jun Zhu. Dpm-solver: A fast ode solver for diffusion probabilistic model sampling in around 10 steps. Advances in Neural Information Processing Systems, 35:5775–5787, 2022.

- [49] Robert B Cleveland, William S Cleveland, Jean E McRae, Irma Terpenning, et al. Stl: A seasonal-trend decomposition. *J. off. Stat*, 6(1):3–73, 1990.
- [50] Lifeng Shen, Weiyu Chen, and James Kwok. Multi-resolution diffusion models for time series forecasting. In *The Twelfth International Conference on Learning Representations*, 2024.
- [51] Jintao Zhang, Mingyue Cheng, Xiaoyu Tao, Zhiding Liu, and Daoyu Wang. Fdf: Flexible decoupled framework for time series forecasting with conditional denoising and polynomial modeling. *arXiv preprint arXiv:2410.13253*, 2024.
- [52] Xinyao Fan, Yueying Wu, Chang Xu, Yuhao Huang, Weiqing Liu, and Jiang Bian. Mg-tds: Multi-granularity time series diffusion models with guided learning process. *arXiv preprint arXiv:2403.05751*, 2024.
- [53] Xinyu Yuan and Yan Qiao. Diffusion-ts: Interpretable diffusion for general time series generation. *arXiv preprint arXiv:2403.01742*, 2024.
- [54] Xinyan Wang, Rui Dai, Kaikui Liu, and Xiangxiang Chu. Effective probabilistic time series forecasting with fourier adaptive noise-separated diffusion. *arXiv preprint arXiv:2505.11306*, 2025.
- [55] Jingwei Liu, Ling Yang, Hongyan Li, and Shenda Hong. Retrieval-augmented diffusion models for time series forecasting. *Advances in Neural Information Processing Systems*, 37:2766–2786, 2024.
- [56] Yushan Jiang, Kanghui Ning, Zijie Pan, Xuyang Shen, Jingchao Ni, Wenchao Yu, Anderson Schneider, Haifeng Chen, Yuriy Nevmyvaka, and Dongjin Song. Multi-modal time series analysis: A tutorial and survey. *arXiv preprint arXiv:2503.13709*, 2025.
- [57] Weilin Ruan, Siru Zhong, Haomin Wen, and Yuxuan Liang. Vision-enhanced time series forecasting via latent diffusion models. *arXiv preprint arXiv:2502.14887*, 2025.
- [58] Chen Su, Yuanhe Tian, and Yan Song. Multimodal conditioned diffusive time series forecasting. *arXiv preprint arXiv:2504.19669*, 2025.
- [59] Yuansan Liu, Sudanthi Wijewickrema, Dongting Hu, Christofer Bester, Stephen O’Leary, and James Bailey. Stochastic diffusion: A diffusion probabilistic model for stochastic time series forecasting. *arXiv preprint arXiv:2406.02827*, 2024.
- [60] Yusuke Tashiro, Jiaming Song, Yang Song, and Stefano Ermon. Csd: Conditional score-based diffusion models for probabilistic time series imputation. *Advances in neural information processing systems*, 34:24804–24816, 2021.
- [61] Yuxin Li, Wenchao Chen, Xinyue Hu, Bo Chen, Mingyuan Zhou, et al. Transformer-modulated diffusion models for probabilistic multivariate time series forecasting. In *The Twelfth International Conference on Learning Representations*, 2024.
- [62] Weiwei Ye, Zhuopeng Xu, and Ning Gui. Non-stationary diffusion for probabilistic time series forecasting. *arXiv preprint arXiv:2505.04278*, 2025.
- [63] Salva Rühling Cachay, Bo Zhao, Hailey Joren, and Rose Yu. Dyffusion: A dynamics-informed diffusion model for spatiotemporal forecasting. *Advances in neural information processing systems*, 36:45259–45287, 2023.
- [64] Lifeng Shen and James Kwok. Non-autoregressive conditional diffusion models for time series prediction. In *International Conference on Machine Learning*, pages 31016–31029. PMLR, 2023.
- [65] Muyao Wang, Wenchao Chen, Zhibin Duan, and Bo Chen. Treating brain-inspired memories as priors for diffusion model to forecast multivariate time series. *arXiv preprint arXiv:2409.18491*, 2024.
- [66] Siyang Li, Yize Chen, and Hui Xiong. Channel-aware contrastive conditional diffusion for multivariate probabilistic time series forecasting. *arXiv preprint arXiv:2410.02168*, 2024.

- [67] Qi Li, Zhenyu Zhang, Lei Yao, Zhaoxia Li, Tianyi Zhong, and Yong Zhang. Diffusion-based decoupled deterministic and uncertain framework for probabilistic multivariate time series forecasting. In The Thirteenth International Conference on Learning Representations, 2025.
- [68] Shiyang Zhou, Zehao Gu, Yun Xiong, Yang Luo, Qiang Wang, and Xiaofeng Gao. Redi: Recurrent diffusion model for probabilistic time series forecasting. In Proceedings of the 33rd ACM International Conference on Information and Knowledge Management, pages 3505–3514, 2024.
- [69] Hao Yang, Zhanbo Feng, Feng Zhou, Robert C Qiu, and Zenan Ling. Series-to-series diffusion bridge model. arXiv preprint arXiv:2411.04491, 2024.
- [70] Guokun Lai, Wei-Cheng Chang, Yiming Yang, and Hanxiao Liu. Modeling long-and short-term temporal patterns with deep neural networks. In The 41st international ACM SIGIR conference on research & development in information retrieval, pages 95–104, 2018.
- [71] Haoyi Zhou, Shanghang Zhang, Jieqi Peng, Shuai Zhang, Jianxin Li, Hui Xiong, and Wancai Zhang. Informer: Beyond efficient transformer for long sequence time-series forecasting. In Proceedings of the AAAI conference on artificial intelligence, volume 35, pages 11106–11115, 2021.
- [72] Spyros Makridakis and Michele Hibon. The m3-competition: results, conclusions and implications. International journal of forecasting, 16(4):451–476, 2000.
- [73] Shengnan Guo, Youfang Lin, Ning Feng, Chao Song, and Huaiyu Wan. Attention based spatial-temporal graph convolutional networks for traffic flow forecasting. In Proceedings of the AAAI conference on artificial intelligence, volume 33, pages 922–929, 2019.
- [74] Chao Chen, Karl Petty, Alexander Skabardonis, Pravin Varaiya, and Zhanfeng Jia. Freeway performance measurement system: mining loop detector data. Transportation research record, 1748(1):96–102, 2001.
- [75] Boyin Huang, Chunying Liu, Viva Banzon, Eric Freeman, Garrett Graham, Bill Hankins, Tom Smith, and Huai-Min Zhang. Improvements of the daily optimum interpolation sea surface temperature (doisst) version 2.1. Journal of Climate, 34(8):2923–2939, 2021.
- [76] Karl Otness, Arvi Gjoka, Joan Bruna, Daniele Panozzo, Benjamin Peherstorfer, Teseo Schneider, and Denis Zorin. An extensible benchmark suite for learning to simulate physical systems. arXiv preprint arXiv:2108.07799, 2021.
- [77] Haoxin Liu, Shangqing Xu, Zhiyuan Zhao, Ling kai Kong, Harshavardhan Kamarthi, Aditya B Sasanur, Megha Sharma, Jiaming Cui, Qingsong Wen, Chao Zhang, et al. Time-mmd: A new multi-domain multimodal dataset for time series analysis. arXiv preprint arXiv:2406.08627, 2024.
- [78] Kai Kim, Howard Tsai, Rajat Sen, Abhimanyu Das, Zihao Zhou, Abhishek Tanpure, Mathew Luo, and Rose Yu. Multi-modal forecaster: Jointly predicting time series and textual data. arXiv preprint arXiv:2411.06735, 2024.
- [79] Geon Lee, Wenchao Yu, Kijung Shin, Wei Cheng, and Haifeng Chen. Timecap: Learning to contextualize, augment, and predict time series events with large language model agents. In Proceedings of the AAAI Conference on Artificial Intelligence, volume 39, pages 18082–18090, 2025.
- [80] Alessandro T Gifford, Kshitij Dwivedi, Gemma Roig, and Radoslaw M Cichy. A large and rich eeg dataset for modeling human visual object recognition. NeuroImage, 264:119754, 2022.